Applied Surface Science 347 (2015) 291–298

Contents lists available at ScienceDirect

Applied Surface Science

journal homepage: www.elsevier.com/locate/apsusc

DFT study of CO adsorption on Pd-SnO_2(1 1 0) surfaces

Pablo Bechthold, María Estela Pronsato, Carolina Pistonesi*

Departamento de Física, Universidad Nacional del Sur & IFISUR (UNS-CONICET), Av. Alem 1253, 8000 Bahía Blanca, Argentina

ARTICLE INFO

Article history:
Received 7 November 2014
Received in revised form 22 March 2015
Accepted 23 March 2015
Available online 17 April 2015

Keywords:
Carbon monoxide
Palladium
Tin oxide
DFT

ABSTRACT

We studied the effect of Pd on the adsorption of CO on the tin oxide surface SnO_2(1 1 0) by Density Functional Theory calculations. Molecular CO adsorbs more strongly in the presence of Pd pre-deposited on the surface. The most stable adsorption sites are those bonded to the Pd atom near a Pd top position on a tilted configuration. In this case the C—O distance increases, producing a weakening of the bond and the calculated stretching frequency decreases. Analysis of the atomic orbital interactions reveals that Pd—CO bonding involves C s - O p and p orbitals from CO, with Pd d orbitals.

For CO sites bonded to Pd, CO bonds to the surface producing a weakening of the surface Pd-O bond.

The electronic configuration analysis shows that in all cases the CO molecule withdraws charge from the surface.

1. Introduction

Metal oxides based semiconductors such as SnO_2 are widely used as gas sensors for many reducing and oxidizing gases [1], operating on the principle that the surface conductivity changes when the gas molecules interact with it [2–4]. Their sensing and catalytic properties depend on grain size, texture, stoichiometry and can be optimised by adding small quantities of transition metals like Pd, Pt or Au [5–8]. However, the interaction of these dopants with the oxide and the gases and its influence on the sensor response is not well understood yet. Both experimental and theoretical contributions have been dedicated to the preparation and characterization of clean and metal doped tin oxide.

Epifani et al. investigated the behaviour of Os, Ni, Pd and Pt doped SnO_2 using thermal analysis and FTIR characterization. It was observed that Pt and Pd were likely to form nanoparticles on the SnO_2 unlike Os and Ni [9]. Infrared studies were also performed on SnO_2 and Pd-SnO_2 catalysts to study the adsorption of CO and NO concluding that the palladium pre-treatment of the sample had a great influence on the species formed on the surface [10].

Recently Hübner et al. studied the influence of Al, Pd and Pt dopants, on the conduction mechanism of SnO_2 by measuring changes in the DC–resistance and work function compared to undoped SnO_2 [11]. X-ray photoelectron spectroscopy (XPS) and secondary ion mass spectroscopy (SSIM) were employed to study the gas sensing properties of Pd ultra-thin films deposited on pyrolytically prepared SnO_x substrates and on SnO_2 powders in real sensing condition, i.e., during heating in air and in hydrogen-enriched air [12,13]. It was shown that reversible oxidation and reduction of Pd occurs during heating. Pd particles supported on SnO_2 oxidize easier and are more difficult to reduce than a Pd(1 1 1) single crystal due to the interaction between the Pd particles and the SnO_2 substrate.

In order to investigate the possible formation of bimetallic phases, Pd particles supported on SnO_2 were studied by X-ray diffraction and transmission and scanning electron microscopy after different reductive treatments by Lorenz et al. [14]. They observed the formation of Pd_2Sn and PdSn at 573 K on the P/SnO_2 on a thin film sample, on the other hand, Pd_3Sn_2 and Pd_2Sn were mainly obtained on a powder catalyst.

Density Functional Theory (DFT) calculations have been employed to predict geometry, electronic structure and energetics of SnO_2 systems [15–18], and to describe vibrational and optical properties [19,20]. DFT has also been used to study the interaction of gases with doped and undoped SnO_2 surfaces. Rantala et al. employed the GGA approximation to describe the (1 1 0) surface band structure [16]. Mäki-Jaskaari and Rantala have also calculated surface formation energies of oxygen deficient SnO_2 (1 1 0) surfaces finding that the stoichiometric surface is the most stable and suggesting that stability decreases with increasing oxygen deficiency [17].

Li et al., using first-principles method based on the density functional theory, have analyzed the oxidation process of CO on Pt-doped SnO_2 [21] finding that Pt substituting Sn on the surface promotes CO oxidation.

* Corresponding author. Tel.: +54 291 4595101x2812; fax: +54 0291 4595142.
E-mail addresses: pbechthold@uns.edu.ar (P. Bechthold), pronsato@criba.edu.ar (M.E. Pronsato), carolina.pistonesi@uns.edu.ar (C. Pistonesi).

http://dx.doi.org/10.1016/j.apsusc.2015.03.149
0169-4332/

Zeng et al. used first principles calculations to study the hydrogen sensing properties of Cr, Cu and Pd doped SnO_2. They showed that Pd/SnO_2 (1 1 0) surface adsorbs the largest amount of H_2 molecules with an electron density transfer from the adsorbed molecule, thus having the potential for improving the sensor response to hydrogen [22].

The aim of this contribution is to investigate CO adsorption on pure and Pd pre-deposited SnO_2 (1 1 0) surfaces using DFT calculations. We report a study of adsorption geometries, electronic structure, charges and bonding.

2. Computational methods and SURFACE models

DFT calculations were performed using the Vienna Ab-Initio Simulation Package (VASP) [23–26] which employs a plane-wave basis set and a periodic supercell method. Potentials within the projector augmented wave (PAW) method [27] and the gradient-corrected functionals in the form of the generalized-gradient approximation (GGA) with the Perdew–Burke–Ernzerhof (PBE) functional [28,29] were used.

The bulk rutile SnO_2 has a tetragonal structure with two SnO_2 units per unit cell. It is composed of six-fold coordinated Sn atoms and three-fold coordinated O atoms.

For bulk optimization, SnO_2 lattice parameters were determined by minimizing the total energy of the unit cell using a conjugated-gradient algorithm to relax the ions [30]. Results for bulk relaxation were checked for convergence with respect to the number of k-points and cutoff energy, concluding that a $5 \times 5 \times 5$ grid and a cutoff energy of 500 eV ensure fully converging results. Larger number of k-points were also considered but the change in the energies was less than 0.02%. The calculated lattice parameters obtained for bulk SnO_2 were $a = 4.81$ Å, $c = 3.22$ Å which are a little higher than experimental values ($a = 4.74$ Å, $c = 3.19$ Å) [31]. Each lattice parameter was overestimated 1.5 and 1.9%. The computed value for the bulk modulus B was 219.6 GPa in full agreement with the 218 GPa experimental value [32].

The energetics of several low-index SnO_2 surfaces has been studied previously by DFT calculations, showing that the (1 1 0) surface is the one with the lowest surface energy [33,34]. The SnO_2 (1 1 0) surface was modelled considering the stoichiometric surface which contains bridging oxygen atoms keeping the composition of bulk SnO_2. The stoichiometric surface is represented using a seven layer slab, three layers containing both Sn and O atoms and six bridging O atoms layer, resulting in a supercell of 13.39 Å by 9.55 Å representing the surface with a thickness of 9.30 Å. The area of the surface is large enough to allow the study of adsorbed species. The vacuum spacing between two repeated slabs is 26.6 Å. During optimization the first two layers were allowed to relax, and a set of $3 \times 3 \times 1$ Monkhorst-Pack k-points was used to sample the Brillouin zone.

The pre-depostion of a Pd atom on the SnO_2 (1 1 0) surface was also considered. During these calculations both the pre-deposited species and the first two surface layers were allowed to relax. Details on surface and bulk optimizations are reported in a previous paper [35]

The adsorption of the CO molecule was investigated on different sites of SnO_2(1 1 0) and Pd-SnO_2(1 1 0) surfaces, with CO coordinated via the C atom to the substrate. In all cases the adsorbate and the first two layers of the slab were fully relaxed.

The CO adsorption energy was computed by subtracting the energies of the gas-phase and surface species from the energy of the adsorbed system as follows

$$E_{ads}(CO) = E(CO/slab) - E(CO_{gas}) - E(slab)$$

With this definition, negative adsorption energy corresponds to an energetically favourable adsorption site on the surface and more negative values correspond to stronger adsorption energies.

Spin polarized calculations were also considered although magnetic effects were found to be negligible in our case. During optimization all atomic coordinates were allowed to relax until a convergence of 1.0 meV for the total energy was reached. In all cases, the cut-off energy was 500 eV.

Density of states (DOS) curves were used to analyse the electronic structure of the system with and without Pd pre-deposited on the surface. For a qualitative study on bonding, the concept of overlap population (OP) as implemented in the YAeHMOP code [36] was applied on the DFT optimized geometries previously presented. A similar procedure was implemented by Papoian et al. [37].

The electronic charges on atoms were computed using Bader analysis [38]. The charge of the CO molecule was calculated adding the individual charges of the C and the O atoms.

3. Results and discussion

3.1. Surface properties

During this study clean stoichiometric SnO_2 (1 1 0) and Pd pre-deposited Pd-SnO_2 (1 1 0) surfaces were analyzed. These surfaces present two types of surface oxygen atoms, two-fold coordinated bridging O atoms (like O1, O4 and O5, see Fig. 1) and three-fold coordinated O atoms (O2, O3 and O6). The removal of the bridging oxygen atoms leads to a non-stoichiometric surface, which corresponds to an oxygen deficient surface termination studied previously [17,35]. Robina et al., in a theoretical study found that Pd clusters are more stable on the stoichiometric surfaces than on non-stoichiometric or reduced SnO_2 (1 1 0) surfaces [35].

The most stable configuration for a Pd atom pre-deposited on the surface corresponds to a Pd atom located at 2.13 Å from its first bridging O neighbour (O1) and equidistant to two surface O (O2, O3), at 2.89 Å and at 2.70 Å from its closest Sn atom (Sn1), as shown in Fig. 1.

Table 1 presents the computed electronic charge for the atoms on both SnO_2 surface (1st column) and on the Pd-SnO_2 surface (3rd column). Charges are expressed in electron charge units. The Pd atom becomes negatively charged (−0.108 e) due to some electron density transfer from its first neighbour O atoms (O1, O2 and O3) which reduce their electron charge. Sn atom close to Pd (Sn1) also reduces its charge (an increase in the positive charge means a decrease on the electron density) which could lead to a redistribution on electron density of the surface (O4 and O5 increase its charge slightly)

In order to analyze the electronic structure Projected DOS curves (PDOS) of atomic orbitals on surface atoms were plotted for Pd-SnO_2 (1 1 0) surface. PDOS of surface Sn atom (Fig. 2-a) shows that there is a band from −20 to −18 eV which comes mainly from s and p contributions, and a band from −9 up to the Fermi level with s contribution on its lower energy part, and mainly p and some d contribution on its higher energy part. For surface O bridging atom close to Pd (Fig. 2-b) the lower energy band corresponds to s states while the higher to p states. Pd contributes mainly with d states near the Fermi level (Fig. 2-c). Comparing the PDOS curves we can conclude that the main interaction between Pd and the surface is through O p and Sn d states.

The interaction of the pre-deposited Pd atom with the substrate was also analyzed using the concept of overlap population (OP) between pairs of atoms before and after Pd pre-deposition. Pd interacts mainly with a bridging O atom. A Pd-O1 bond is formed with an OP value of 0.210, affecting the bonding of its nearest

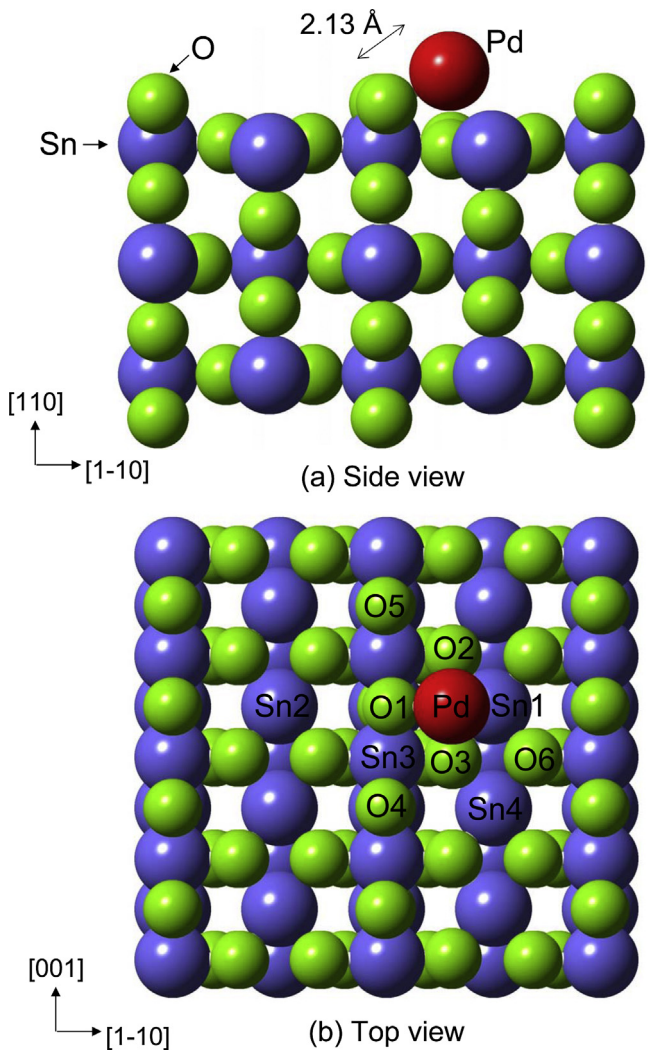

Fig. 1. Surface structure of Pd-SnO_2 (1 1 0) surface side (a) and top (b) views.

neighbours. The OP between Sn3 and O1 near the palladium atom decreases from 0.320 to 0.280 (around 12%), indicating a weakening of the Sn-O bond. Also Sn1-O3 overlap population decreases from 0.315 to 0.289 (8%), so the Pd-O1 bond forms mainly at expense of the Sn—O bond weakening. Finally we notice that there is an OP value of 0.061 for Pd-Sn1 atoms, although is a small value is not negligible, indicating also a small Pd—Sn interaction as represented in PDOS curves.

3.2. CO adsorption on clean SnO_2(1 1 0) surfaces

CO adsorption on clean SnO_2 surface was analyzed on several adsorption sites. According to our calculations the CO molecule preferentially adsorbs on Sn top sites with the C atom pointing towards the surface (Fig. 3). For this site the adsorption energy is −0.56 eV with a C—O distance of 1.14 Å which results similar to that in the isolated CO molecule. The C-Sn distance is 2.50 Å.

Li et al., using first-principles methods based on the density functional theory, [21] also found that the most stable configuration for the CO adsorption on this surface corresponds to the CO adsorbed on top of Sn site with an adsorption energy of 0.43 eV, with C—Sn and C—O distances of 2.48 Å and 1.15 Å, respectively. Weigen et al. by means of DFT calculations, also concluded that carbon monoxide adsorbed on SnO_2 (1 1 0) surface with C end on a Sn atom site, is the most energetically stable adsorption position [39]. IR experiments performed by Almaric et al. [10] at low CO pressure on SnO_2, show bands in the 2500–2000 cm^{-1} range, attributed to "on-top" CO—Sn entities.

When CO is adsorbed on top of Sn, the electron charge of Sn2 atom decreases by 0.121 e (compare 1st and 2nd columns of Table 1). As a result, the surface transfers charge to the CO molecule, making it negatively charged with a net charge of −0.122 e.

The calculated C-O stretching frequency is 2144 cm^{-1}. These results are in agreement with FTIR studies of SnO_2 samples at 120 K at low CO pressures which showed an adsorption band at 2210-2196 cm^{-1} associated to CO bound to a coordinational unsaturated Sn^{4+} surface species [40].

Table 2 shows OP values and distances for this system. The OP value for the surface Sn-O bond reduces after CO adsorption and the C—Sn OP value becomes 0.231. We can conclude that C—Sn bond forms at expenses of Sn—O weakening. The OP value for the C—O bond is 1.314 (only 2% lower than the corresponding value for the isolated CO molecule).

Comparing the PDOS of the atomic orbitals on Sn atom when CO is adsorbed on top (Fig. 4-b) with the PDOS of the same atoms on the clean surface (Fig. 4-a), we can see that a new peak appears at −9 eV on the s band after CO adsorption. Also for the p band the more intense peak at −5.5 eV becomes stabilized after adsorption, as is clearly seen by the shift of the peak to −6 eV.

Fig. 4-c shows PDOS of atomic orbitals of C (filled line) and O (from CO, dotted line) atoms. There is a sharp band from about −9 to −8 eV composed mainly by O p and C s contributions. The other

Table 1
Net charges for specific atoms on the surface and on adsorbed CO molecule. Al charges are in electron unit charge e. Atoms labels are indicated in Fig. 1.

Electronic charges (Bader)		SnO_2		Pd-SnO_2			
		Isolated SnO_2	CO/SnO_2	Isolated Pd-SnO_2	CO bonded to Pd	CO laterally bonded to Pd	CO on Sn top
Bridging O	O1	−1.749	−1.754	−1.678	−1.730	−1.707	−1.676
	O4	−1.749	−1.761	−1.777	−1.769	−1.759	−1.750
	O5	−1.749	−1.780	−1.760	−1.752	−1.772	−1.764
Surface O	O8	−2.006	−2.062	−2.046	−2.045	−2.068	−2.053
	O7	−2.066	−2.003	−1.999	−1.997	−2.013	−1.991
	O2	−2.066	−2.053	−1.999	−2.005	−1.996	−1.995
	O3	−2.066	−2.067	−1.998	−2.005	−1.983	−1.994
	O6	−2.066	−2.004	−2.041	−2.040	−2.012	−2.039
Sn	Sn2	3.879	4.000	3.882	3.882	3.882	4.000
	Sn1	3.879	3.885	4.000	4.000	4.000	4.000
	Sn4	3.879	3.885	3.870	3.868	3.824	3.868
	Sn3	4.000	4.000	4.000	4.000	4.000	4.000
Pd		–	–	−0.108	−0.027	−0.012	−0.145
O (from CO)		–	−1.785	–	−1.833	−1.785	−1.810
C		–	1.663	–	1.713	1.573	1.684
CO		–	−0.122	–	−0.125	−0.212	−0.127

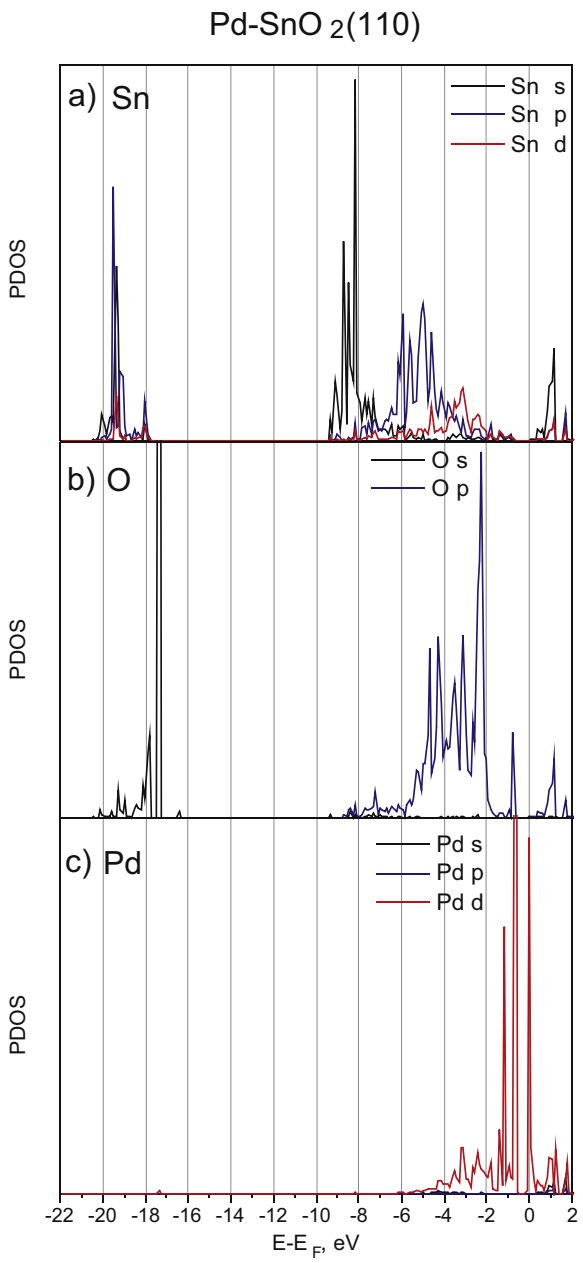

Fig. 2. PDOS on atomic orbitals of surface atoms from Pd-SnO_2 (1 1 0) surface: Sn (a) and bridging O (b) atoms close to Pd (specifically Sn1 and O1, see Fig. 1), and on Pd (c).

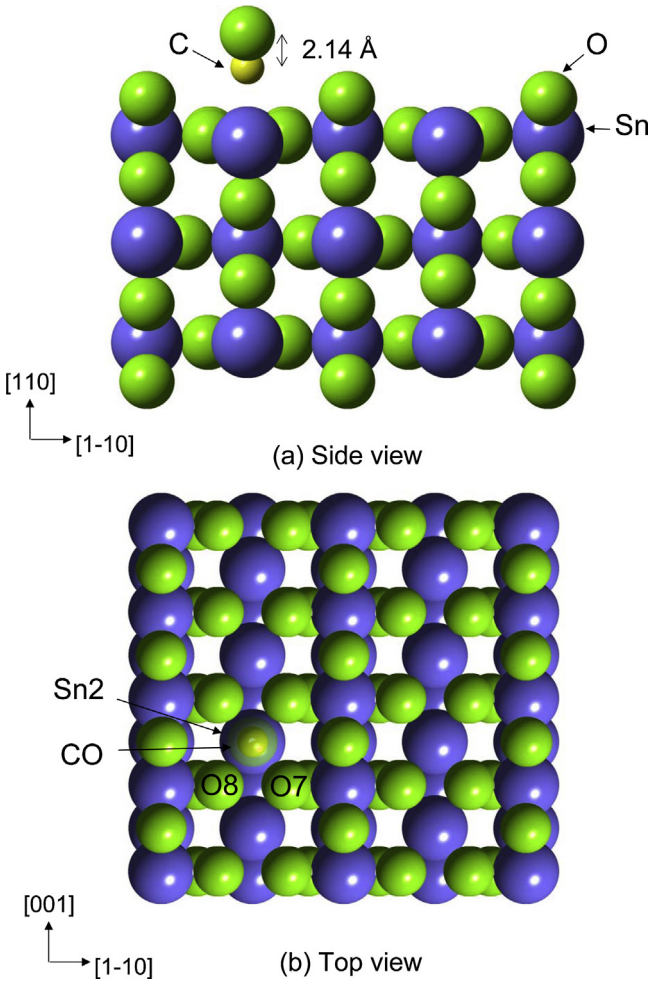

Fig. 3. Surface structure of CO adsorption on SnO_2 (1 1 0) surface side (a) and top (b) views.

Table 2
Interatomic distances and overlap population for relevant bonds for isolated SnO_2 surface and CO molecule, and for adsorbed CO/SnO_2.

	SnO_2		CO		CO/SnO_2	
	Dist., Å	OP	Dist., Å	OP	Dist., Å	OP
C—O	–	–	1.14	1.339	1.14	1.314
C—Sn2	–	–	–	–	2.50	0.231
Sn—O7	2.04	0.306	–	–	2.05	0.294
Sn—O8	2.04	0.315	–	–	2.05	0.287

band from −6.5 to −5 eV corresponds to p contributions of both atoms.

We can conclude that CO bonding to the surface is mainly due to C s and O p interactions with Sn s states (−9 eV) and also with Sn p states interacting with CO p states (−6 eV). Weigen et al. [39] have obtained similar DOS curves which also imply a strong interaction between the molecular orbitals of the CO molecule and atomic orbitals of the Sn atom.

3.3. CO adsorption on Pd-SnO_2 surfaces

CO adsorption was also analyzed on Pd-SnO_2 surface. The preferential adsorption site corresponds to the CO molecule bonded to the Pd atom (Fig. 5-a,b). This is a tilted configuration, the angle formed by the CO molecule with the normal to the surface is 23° and the molecule is slightly shifted from the exact Pd top position and remains far from the surface. Due to CO interaction the Pd atom gets closer to the bridging oxygen atom (Pd-O1 distance reduces 0.05 Å, see Table 3) and it is 0.12 Å further from the surface. The C-O distance increases to 1.15 Å. The Pd-C distance is 1.83 Å, which is shorter than C-Sn distance (2.5 Å) for CO adsorbed on top on clean SnO_2 surface. The adsorption energy is −2.34 eV, corresponding to a stronger adsorption than compared with the clean surface (−0.56 eV).

A comparison with the PdCO molecule and Pd_nCO (n = 1–9) is relevant. The gas phase experimental study of this molecule found Pd-C and C—O distances of 1.845 Å and 1.137 Å, respectively [41]. Zanti and Peeters presented a DFT study of small Pd_n clusters (n = 1–9)-CO [42]. Their results (d_{Pd-C} = 1.867 and d_{C-O} = 1.138 Å) are close to our present calculations when n = 1. Kalita and Deca reported a Pd-CO distance and C—O bond length in neutral and charged Pd_1CO of 1.868 and 1.161 Å, respectively [43]. Similar

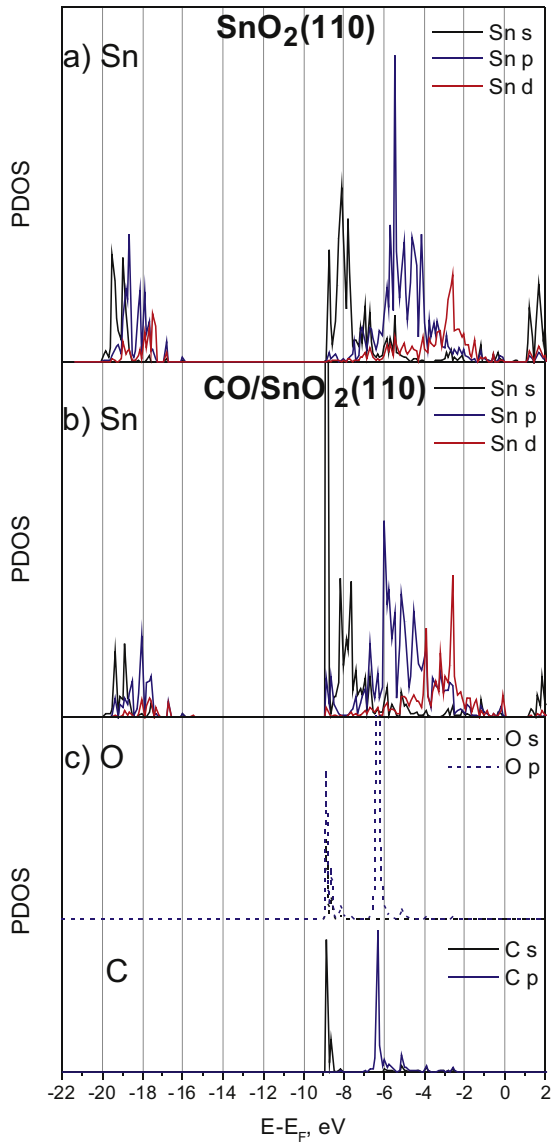

Fig. 4. PDOS on atomic orbitals of surface atoms from Pd-SnO_2 (1 1 0) surface: Sn (a) and bridging O (b) atoms close to Pd, specifically Sn1 and O1, and on Pd (c).

results were also obtained previously by our group for CO adsorption on a PdGa intermetallic compound by DFT calculations, in which the CO adsorbs atop of a Pd atom with a small tilt of 7.8° in the (1 0 0) plane and with Pd—C and C—O distances of 1.961 Å and 1.156 Å, respectively [44].

The next site in order of preference is laterally bonded to the Pd atom (Fig. 5-c,d), having an adsorption energy of −1.01 eV. This is also a tilted configuration with the CO molecule forming an angle of 37° with the normal to the surface. For this configuration the Pd atom is moved away 0.12 Å from its original position towards the C atom. The C—O distance has a further increase to 1.17 Å corresponding to a larger stretch of the molecule. For this configuration the CO molecule is 0.19 Å further from the Pd atom than in the pervious site but it is closer to the surface, specifically C-Sn4 distance is 2.99 Å and C-O6 is 2.92 Å.

These results are in agreement with XPS spectra of samples of Pd-SnO_2 that showed an enhancement of the C—O signal with respect to pure SnO_2 samples. This could be explained in terms of CO molecular adsorption on Pd particles [45].

The adsorption energies of our two models are −2.34 eV and −1.01 eV, respectively, which are much larger than the value (−0.56 eV) calculated on the undoped surface. The results indicate that the doping of Pd increases the active center sites of the surface, so that more CO can be adsorbed easily. This is helpful to increase the sensitivity to CO. These theoretical findings verify the experimental results that Pd doping can improve the sensitivity of CO on SnO_2 surface for gas sensors.

Hu et al., studying a nanocomposite Pd/SnO_2/CNT sensor to detect carbon monoxide, found that the sensitivity of the materials was improved by 80 times relative to that of pure tin oxide at a CO concentration of 500 ppm. Such behavior may be attributed to the catalytic activity of the PdO nanoparticles, the active reaction site, and the enhanced chemisorption and dissociation of the gas [46].

Finally the third site in energy corresponds to a Sn top geometry. This configuration results very similar to that of the CO adsorption on the clean surface, but with an adsorption energy of −0.63 eV (11% higher than on the clean surface). Although the Pd atom is not very close to the CO, it has a stabilization effect.

Regarding the charge transfer, in all cases the surface transfers charge to the CO molecule, making it negatively charged (see the last three columns of Table 1). When CO is bonded to the Pd atom, Pd atom reduces its charge by 0.08 e (compare 4th and 3rd columns of Table 1). The bridging oxygen atom first neighbour to Pd (O1) increases its charge by 0.052 e, also second neighbour O atoms (O2 and O3) have a small increase in their charges (while other bridging oxygen atoms have a small reduction on its charge) and the CO molecule results with a negative charge of −0.125 e. We can conclude that the Pd atom transfers electron density to its first neighbours, especially to the CO molecule.

When CO is bonded laterally to Pd atom there is a further reduction of 0.096 e on the Pd atom charge, and also the closest oxygen atoms to CO, O3 and O6, reduce their charge by 0.015 and 0.029 e respectively. We can conclude that there is more charge transfer to the CO molecule, not only from the Pd but also from the surface O atoms, resulting in a charge of −0.212 e for the CO molecule, which is higher than in the previous case. The CO molecule is closer to the surface thus facilitating extra charge transfer from surface O atoms.

Finally, for CO adsorption on top of Sn, the electron charge of Sn2 atom decreases to 0.118 e, resulting in a net charge of −0.127 e for the CO molecule. These results are similar to that of the CO adsorption on top of Sn atom on clean SnO_2 surface, but in this case bridging oxygen atoms reduce their charge and Pd atom increases its charge to −0.145 e.

The OP value for the C—O bond when the molecule is bonded to a Pd atom is slightly reduced with respect to the corresponding value of the isolated molecule, which is also in agreement with the small elongation of the molecule bond length. There is an OP value of 0.712 for the C—Pd bond and a small reduction of the OP value of the Pd—Sn and Pd—O bonds between Pd and the surface.

For the CO bonded laterally to Pd, although the C—O bond is slightly elongated, the OP value for the bond is higher than in the previous case, this could be associated with the increment on the electron density of the molecule. In this case there is also a weak interaction between C and Sn4 resulting a OP value of 0.074 for the C—Sn4 bond and a reduction of 50% of OP value for the C—Pd bond with respect to the value for the CO bonded to Pd. There is also a higher reduction on the OP value for the Pd—O1 bond. So in both cases (bonded and laterally bonded to Pd) we can conclude that CO bonds to the surface producing a weakening on the Pd—O1 bond.

Finally, when CO is on top of a Sn atom close to Pd the results are qualitatively similar to that of the adsorption on the clean surface. The OP values for the surface Sn—O bonds close to CO present a higher reduction from 0.306 to 0.274 (not shown in Table 3) after CO

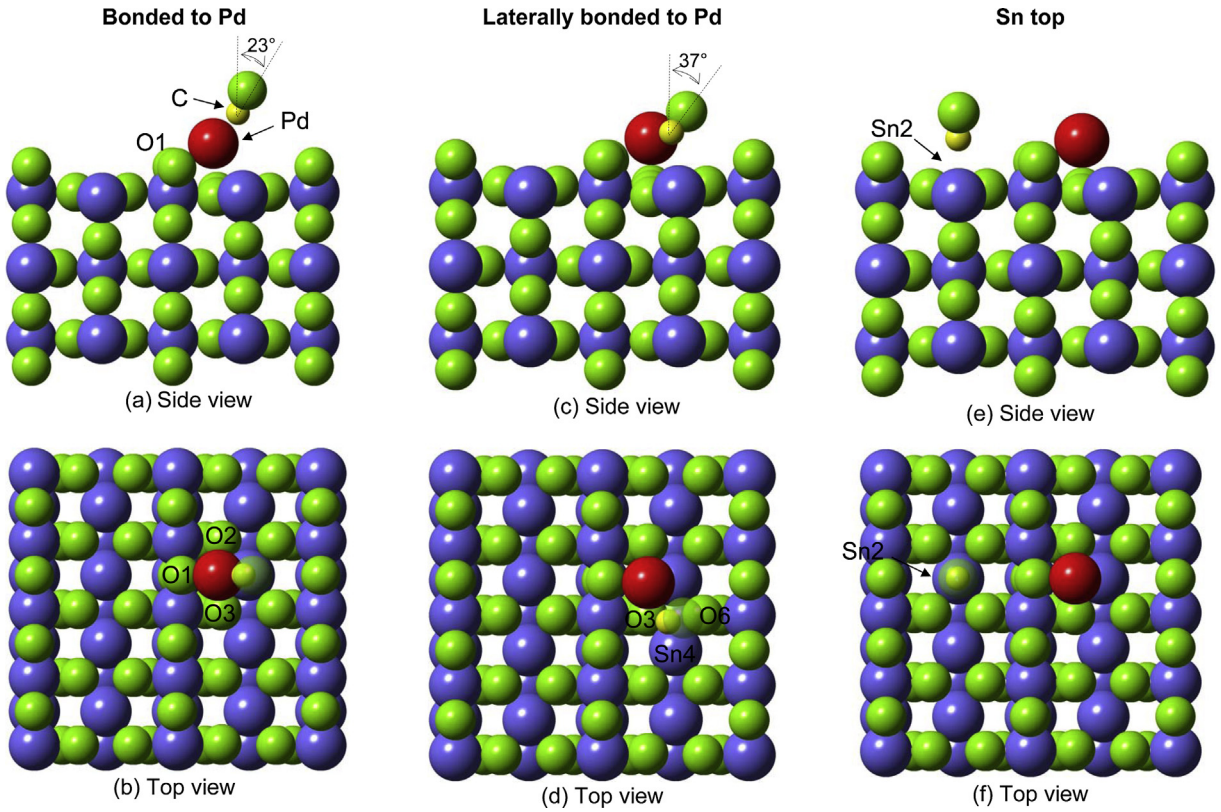

Fig. 5. Surface structure of CO adsorption on Pd-SnO_2 (1 1 0) surface bonded to Pd (a, b), laterally bonded to Pd (c, d) and on Sn top (e, f) side and top views, respectively.

adsorption and the C—Sn OP value increases 50%, so the interaction with the surface becomes stronger in the presence of Pd.

PDOS curves were analyzed only for the most stable site when CO is bonded to the Pd atom. PDOS of Pd atom after CO adsorption (red line, Fig. 6) shows new d peaks at around -8.5 and −6 eV (compare with PDOS before CO adsorption, Fig. 2-c), which could contribute to the stabilization of the system.

Fig. 6 also shows PDOS of atomic orbitals of C (filled line) and O (from CO, dotted line shifted upwards for clarity) atoms. There is a sharp band near −8 eV composed mainly by C s and O p contributions. The other band from −6.5 to −5 eV corresponds to p contributions of both atoms. We can conclude that CO bonding to the surface is due to C s and O p (∼−8 eV), and C and O p (band from −6.5 to −5 eV) interacting with Pd d states.

Table 3 also includes the calculated C—O stretching frequencies. The stretching vibrational mode for the isolated molecule is 2125 cm^{-1}. Pre-deposited Pd produces a shift to lower frequency values when CO is bonded to Pd. This is in agreement with the

Table 3
Interatomic distances and overlap population for relevant bonds for isolated Pd-SnO_2 surface and CO molecule, and for adsorbed CO/SnO_2 on different sites. C-O vibrational frequencies are also included.

	Isolated CO Isolated Pd -SnO_2		CO/Pd -SnO_2					
			Bonded to Pd E_{ads} = −2.34 eV		Laterally bonded to Pd E_{ads} = −1.01 eV		Sn top E_{ads} = −0.63 eV	
	Dist., Å	OP	Dist., Å	OP	Dist. (Å)	OP	Dist. (Å)	OP
C—O	1.14	1.339	1.15	1.240	1.17	1.274	1.14	1.356
C—Pd	–	–	1.83	0.712	2.02	0.354	–	–
C—Sn	–	–	–	–	[a]2.99	0.074	2.52	0.351
C-O6	–	–	–	–	2.92	–	–	–
Pd—Sn1	2.70	0.061	2.83	0.053	2.83	0.074	2.66	0.078
Pd—O1	2.13	0.208	2.08	0.201	2.66	0.185	2.12	0.201
Pd—O2	2.89	–	3.02	–	2.95	–	2.89	–
Pd—O3	2.89	–	3.02	–	3.03	–	2.89	–
ν_{CO}, cm^{-1}	2125	2086	1870	2164 ([b]2144)				

[a] C-Sn4.
[b] For CO on Sn top on SnO_2 surface (without Pd).

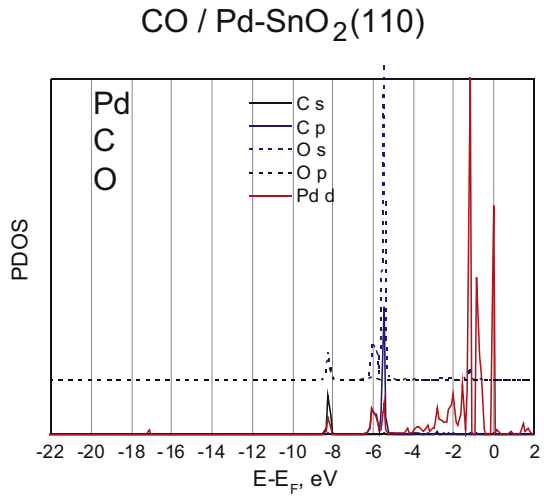

Fig. 6. PDOS on atomic orbitals of C and O atoms from CO and also Pd atom for CO/Pd-SnO_2 (1 1 0) surface.

elongation and weakening of the C—O bond. The frequency is even lower for CO bonded laterally to Pd, which has a higher C—O distance. The calculated frequency values of 2086 and 1870 cm^{-1} for CO bonded and laterally bonded to Pd are in agreement with experimental results using polarization modulation infrared reflection spectroscopy (PM-IRAS) combining with Scanning Tunnelling Spectroscopy (STM) to study CO adsorption on Pd-nanoclusters deposited on crystalline SiO_2 thin films, which yield two bands at 2089 and 1957 cm^{-1} when CO is adsorbed: the first band have been assigned to CO adsorbed on-top and the other band was assigned to CO molecules occupying bridges sites, possible near some defects like steps [47].

When CO is on top of Sn, the stretching frequency is slightly higher than that of the isolated molecule, although C—O distance is similar, the C—O bond is stronger than that of the isolated molecule, as indicated by the increase of the OP value.

Finally, Pd doping also causes the shift of the Fermi level, which corresponds to an increase of 0.77 eV compared to the undoped surface. In addition, a significant difference is that peaks on PDOS curves associated with the surface states appear in the band gap of the undoped surface (compare Fig. 2-c with Fig. 4). These peaks are mainly composed of the Pd 4d orbital states. It is interesting to note that the band structure of the doped model has a significant difference with respect to the undoped one: for the clean SnO_2 surface PDOS curves (Fig. 4) show a band gap of around 1 eV, as was reported in a previous paper [35]. On the other hand, when Pd predeposited PDOS curves are analyzed (Fig. 2), the plots show some unoccupied Pd d states above the Fermi level. No band gap is now observed when Pd is on the surface. The additional states caused by Pd doping are the main reason for the change in the electronic structure of SnO_2 (1 1 0) surface.

Thus, palladium seems to either influence the electronic structure as a whole and creates new adsorption sites in the SnO_2 lattice that leads to enhanced selectivity and sensitivity. There are more electrons in the conduction band of SnO_2 which contribute to the increased sensor signals.

The main finding in our theoretical study is that Pd-SnO_2 (1 1 0) surfaces can be useful as gas sensors due to the presence of more stable Pd adsorption sites on the surface that could improve CO gas adsorption.

Semiconducting metal oxide sensors are one of the most widely studied groups of gas sensors, a review is presented on reference [48]. Specifically Pd-SnO_2 based sensors, may be useful for the selective detection of pollutants, in particular CO.

4. Conclusions

The adsorption of CO on clean SnO_2(1 1 0) and on Pd-SnO_2 surfaces were computed using periodic DFT calculations. The adsorption of CO is energetically more favourable in the presence of Pd pre-deposited on the surface. The most stable adsorption sites are those with the C atom bonded to Pd, on a tilted configuration, near a Pd top position. In this case the C—O distance increases producing a weakening of the bond and the calculated stretching frequency decreases when compared with the isolated molecule. Analysis of the atomic orbital interactions reveals that Pd—CO bonding involves C s—O p and p orbitals from CO, with Pd d orbitals.

In all cases CO bonds to the surface with the C atom pointing towards the surface. A C-surface bond is formed producing a weakening of its first neighbours surface bonds: there is a reduction on surface Sn—O bond when CO is bonded on top of a Sn site (on clean and on Pd doped surface) and a weakening on surface Pd—O bond when CO is bonded to a Pd atom.

Also for all configurations under study, the CO molecule withdraws charge from the surface, resulting a negatively charged molecule.

It was found that Pd doping can enhance CO adsorption, these theoretical findings are in agreement with the XPS results that Pd doping increases CO signals.

Acknowledgment

The authors are grateful for the financial support from PICT 1770, MINCyT-ARC/13/11, SGCyT-UNS PGI 24/F048. C.P and M.E.P. are members of CONICET, P.Bechthold is a fellow researcher at this Institution.

References

[1] M. Batzill, U. Diebold, The surface and materials science of tin oxide, Pro. Surf. Sci. 79 (2005) 47–154.
[2] W. Göpel, K.D. Schierbaum, SnO_2 sensors: current status and future prospects, Sens. Actuators B 26 (1995) 1–12.
[3] B. Ruhland, T. Becker, G. Muller, Gas-kinetic interactions of nitrous oxides with SnO_2 surfaces, Sens. Actuators B 50 (1998) 85–94.
[4] H. Ohnishi, H. Sasaki, T. Matsumoto, M. Ippommatsu, Sensing mechanism of SnO2 thin film gas sensors, Sens. Actuators B 14 (1993) 677–678.
[5] A. Cabot, A. Vilà, J.R. Morante, Analysis of the catalytic activity and electrical characteristics of different modified SnO_2 layers for gas sensors, Sens. Actuators B 84 (2002) 12–20.
[6] A. Chiorino, G. Ghiotti, M.C. Carotta, G. Martinelli, Electrical and spectroscopic characterization of SnO_2 and Pd-SnO_2 thick films studied as CO gas sensors, Sens. Actuators B 47 (1998) 205–212.
[7] W. Li, C. Shen, G. Wu, Y. Ma, Z. Gao, X. Xia, G. Du, New model for a Pd-doped SnO_2-based CO gas sensor and catalyst studied by online in-situ x-ray photoelectron spectroscopy, J. Phys. Chem. C 115 (2011) 21258–21263.
[8] J. Kappler, N. Barsan, U. Weimar, A. Dièguez, J.L. Alay, A. Romano–Rodriguez, J.R. Morante, W. Göpel, J. Fresen, Correlation between XPS, Raman and TEM measurements and the gas sensitivity of Pt and Pd doped SnO_2 based gas sensors, Anal. Chem. 361 (1998) 110–114.
[9] M. Epifani, M. Alvisi, L. Mirenghi, G. Leo, P. Siciliano, L. Vasanelli, Sol-gel processing and characterization of pure and metal-doped SnO_2 thin films, J. Am. Ceram. Soc. 84 (1) (2001) 48–54.
[10] D. Amalric-Popescu, F. Bozon-Verduraz, Infrared studies on SnO_2 and Pd/SnO_2, Cat. Today 70 (2001) 139–154.
[11] M. Hübner, N. Bârsan, U. Weimar, Influences of Al, Pd and Pt additives on the conduction mechanism as well as the surface and bulk properties of SnO_2 based polycrystalline thick film gas sensors, Sens. Actuators B 171–172 (2012) 172–180.
[12] T. Skála, K. Veltruská, M. Moroseac, I. Matolínová, A. Cirera, V. Matolín, Redox process of Pd-SnO_2 system, Surf. Sci. 566–568 (2004) 1217–1221.
[13] M. Moroseac, T. Skála, K. Veltruská, V. Matolín, I. Matolínová, XPS and SSIMS studies of Pd/SnOx system: Reduction and oxidation in hydrogen containing air, Surf. Sci. 566–568 (2004) 1118–1123.
[14] H. Lorenz, Q. Zhao, S. Turner, O.I. Lebedev, G. Van Tendeloo, B. Klötzer, C. Rameshan, K. Pfaller, J. Konzett, S. Penner, Origin of different deactivation of Pd/SnO_2 and Pd/GeO_2 catalysts in methanol dehydrogenation and reforming: A comparative study, App. Catal. A Gen. 381 (2010) 242–252.

[15] I. Manassidis, J. Gonniakowski, L.N. Kantorovich, M.J. Gillan, The structure of the stoichiometric and reduced SnO2(110) surface, Surf. Sci. 339 (1995) 258–271.
[16] T.T. Rantala, T.S. Rantala, V. Lantto, Electronic structure of SnO2 (110) surface, Mat. Sci. Sem. Proc. 3 (2000) 103–107.
[17] M.A. Mäki-Jaskari, T.T. Rantala, Theoretical study of oxygen-deficient SnO_2(110) surfaces, Phys. Rev. B 65 (2002) 1–8, 245428.
[18] M.A. Mäki-Jaskari, T.T. Rantala, Density functional study of Pd adsorbates at SnO_2(1 1 0) surfaces, Surf. Sci. 537 (2003) 168–178.
[19] P.D. Borges, L.M.R. Scolfaro, H.W. Leite Alves, E.R. da Silva Jr., DFT study of the electronic, vibrational, and optical properties of SnO_2, Theor. Chem. Acc. 126 (2010) 39–44.
[20] W. Liu, Z. Liu, L. Feng, First-principles calculations of structural, electronic and optical properties of tetragonal SnO_2 and SnO, Comput. Mat. Sci. 47 (2010) 1016–1022.
[21] S. Li, Z. Lu, Z. Yang, X. Chu, The sensing mechanism of Pt-doped SnO_2 surface toward CO: A first-principle study, Sens. Actuators B 202 (2014) 83–92.
[22] W. Zeng, T. Liu, D. Liu, E. Han, Hydrogen sensing and mechanism of M-doped SnO_2 (M = Cr^{3+}, Cu^{2+} and Pd^{2+}) nanocomposite, Sens. Actuators B 160 (2011) 455–462.
[23] G. Kresse, J. Hafner, Ab initio molecular dynamics for open-shell transition metals, Phys. Rev. B 48 (1993) 13115–13118.
[24] G. Kresse, J. Hafner, Ab initio molecular-dynamics simulation of the liquid-metal-amorphous-semiconductor transition in germanium, Phys. Rev. B. 49 (1994) 14251–14269.
[25] G. Kresse, J. Furthmv̈ller, Efficiency of ab-initio total energy calculations for metals and semiconductors using a plane-wave basis set, Comput. Mater. Sci. 6 (1996) 15–50.
[26] G. Kresse, J. Furthmv̈ller, Efficient iterative schemes for ab initio total-energy calculations using a plane-wave basis set, Phys. Rev. B 54 (1996) 11169–11186.
[27] G. Kresse, D. Joubert, From ultrasoft pseudopotentials to the projector augmented-wave method, Phys. Rev. B 59 (1999) 1758–1775.
[28] J.P. Perdew, K. Burke, M. Ernzerhof, Generalized gradient approximation made simple, Phys. Rev. Lett. 77 (1996) 3865–3868.
[29] J.P. Perdew, K. Burke, M. Ernzerhof, Generalized gradient approximation made simple, Phys. Rev. Lett. 78 (1997) 1396.
[30] W.H. Press, B.P. Flannery, S.A. Teukolsky, W.T. Vetterling, Numerical Recipes, Cambridge University Press, New York, 1986.
[31] A.A. Bolzan, C. Fong, B.J. Kennedy, C.J. Howard, Structural studies of rutile-type metal dioxides, Acta Crystallogr. Sect. B e Struct. Sci. 53 (1997) 373–380.
[32] R.M. Hazen, L.W. Finger, Bulk moduli and high-pressure crystal structures of rutile-type compounds, J. Phys. Chem. Solids 42 (1981) 143–151.
[33] J. Oviedo, M.J. Gillan, Energetics and structure of stoichiometric SnO_2 surfaces studied by first-principles calculations, Surf. Sci. 463 (2000) 93–101.
[34] J.D. Prades, A. Cirera, J.R. Morante, J.M. Runeda, P. Ordejón, Ab initio study of NOx compounds adsorption on SnO_2 surface, Sens. Actuators B 126 (2007) 62–67.
[35] A. Robina, E. Germán, M.E. Pronsato, A. Juan, I. Matolínová, V. Matolín, Electronic structure and bonding of small Pd clusters on the stoichiometric and reduced SnO_2(110) surface, Vacuum 106 (2014) 86–93.
[36] G. Landrum, W. Glassey, Yet Another Extended Hückel Molecular Orbital Package. (YAeHMOP), Cornell University, New York, 1997, http://yaehmop.sourceforge.net
[37] G. Papoian, J.K. Norskov, R. Hoffmann, A comparative study of hydrogen, methyl, and ethyl chemisorption on the Pt (111) surface, J. Am. Chem. Soc. 122 (2000) 4129–4144.
[38] W. Tang, E. Sanville, G. Henkelman, A grid-based Bader analysis algorithm without lattice bias, J. Phys. Condens. Matter 21 (2009) 84204–84210.
[39] W. Chen, Q. Zhou, F. Wan, T. Gao, Gas sensing properties and mechanism of nano-SnO_2-based sensor for hydrogen and carbon monoxide, J. Nanomat. 2012 (2012) 1–9.
[40] N. Sergent, P. Gélin, L. Périer-Camby, H. Praliaud, G. Thomas, FTIR study of low-temperature CO adsorption on high surface area tin(IV) oxide: probing Lewis and Bronsted acidity, Phys. Chem. Chem. Phys. 4 (2002) 4802–4808.
[41] N.R.J. Walker, K.-H. Hui, C.L. Gerry, Microwave spectrum, geometry, and hyperfine constants of Pdco, J. Phys. Chem. A 106 (2002) 5803–5808.
[42] G. Zanti, D. Peeters, DFT study of small palladium clusters Pd_n and their interaction with a CO ligand (n = 1–9), Eur. J. Inorg. Chem. 26 (2009) 3904–3911.
[43] B. Kalita, R.C. Deka, DFT study of CO adsorption on neutral and charged Pd_n (n = 1–7) clusters, Eur. Phys. J. D 53 (2009) 51–58.
[44] P. Bechthold, J.S. Ardhengi, A. Juan, E.A. González, P.V. Jasen, CO adsorption on PdGa(100), (111) and ($\bar{1}\bar{1}\bar{1}$) surfaces: A DFT study, Appl. Surf. Sci. 315 (2014) 467–474.
[45] K. Veltruská, N. Tsud, V. Brinzari, G. Korotcnkov, V. Matolín, CO adsorption on Pd clusters deposited on pyrolytically prepared SnO_2 studied by XPS, Vacuum 61 (2001) 129–134.
[46] Q. A. Hu, S. A. Liu, Y. B. Lian, Sensors for carbon monoxide based on Pd/SnO_2/CNT nanocomposites, (2014) Physica Status Solidi (A) Applications and Materials Science,. Article in Press.
[47] E. Ozensoy, B.K. Min, A.K. Santra, D.W. Goodman, CO dissociation at elevated pressures on supported Pd nano-clusters, J. Phys. Chem. B 108 (2004) 4351.
[48] S.M. Kanan, O.M. El-Kadri, I.A. Abu-Yousef, M.C. Kanan, Semiconducting metal oxide based sensors for selective gas pollutant detection, Sensors 9 (2009) 8158–8196.